



## Adsorption of anionic, cationic and disperse dyes with activated pyrolytic tire char

Duangkamol Danwanichakul and Panu Danwanichakul\*

Center of Excellence on Natural Rubber Technology, Department of Chemical Engineering, Faculty of Engineering, Thammasat University, Pathumthani, 12120, Thailand

Received April 2015  
Accepted June 2015

### Abstract

Activated pyrolytic tire char was applied as adsorbents to remove dyes from contaminated water. The method of surface treatment with ethanol solution, HCl solution and then activation with NaOH solution was proposed. After activation at 750°C, the specific surface area (SSA) of activated char (AC) increased from 154.7 m<sup>2</sup>/g to 228.9 m<sup>2</sup>/g. The pore size increased slightly from 323.4 Å to 349.3 Å and iodine number increased from 95 mg/g to 137 mg/g. AC was then utilized in the adsorption of three dyes which were acid dye (AR131), basic dye (BR18) and disperse dye (DR167) in a shaker with a speed of 75 rpm at 26°C. The initial concentration was varied to be 10 – 50 mg/L. The kinetic results were more consistent with pseudo-second-order model. Considering the adsorption rate constant,  $k_2$ , it was found that kinetics for acid dye (AR131) was slower than basic dye (BR18) while kinetics for disperse dye (DR167) did not follow specific pattern since it cannot be dispersed well in water without any dispersing agent. Regarding adsorption equilibrium when the initial concentration was between 10-50 mg/L, the adsorption percentages for acid dye (AR131), basic dye (BR18) and disperse dye (DR167) were 88.2 - 100%, 100%, and 26.9 – 50.7%, respectively. In addition, the adsorption isotherms for acid dye (AR131) and basic dye (BR18) followed the Langmuir equation, whereas, that for disperse dye (DR167) was better fit with the Freundlich equation.

**Keywords:** Adsorption, Anionic dye, Cationic dye, Disperse dye, Activated pyrolytic tire char

### 1. Introduction

At present, a very large amount of waste water is generated from textile industry so the large volume of non-biodegradable color could cause serious environmental problems. There are several methods to solve these problems including adsorption. Many adsorbents such as chitosan [1], montmorillonite clay [2], activated carbon [3-4] have been investigated for their efficiencies. The latter choice could be produced from biomass wastes and waste tire rubber [5-7]. One of these work investigated the use of activated carbon derived from waste bamboo culms in the adsorption of azo disperse dye [7].

Pyrolysis is another popular solution to eliminate waste tire rubbers by breaking down rubber molecules at a high temperature without using oxygen. Pyrolytic tire char is composed of about 70-80% fixed carbon and about 13% ash which could be ZnO, silica, sulfur and others. Pyrolytic char has been used as conductive filler in rubber for sensor application [8] and as an effective adsorbent after oxygenated reaction [9-10]. Only a few work reported the use of pyrolytic tire char in removing dyes in water. Mui et al. [11] studied pyrolysis of waste tire at 473-973°C and found that the temperature should not be greater than 573°C since the surface

area of the char would be reduced. The surface treatment was then introduced by treating the char with nitric acid to make the surface more hydrophilic before being used to remove Acid Yellow 117. In another work by the same group [6], the char was further activated with CO<sub>2</sub> to increase its surface area at a very high temperature ranging between 823-1123°C and was used to remove the same dye and methylene blue.

In this work, the pyrolytic char was obtained at temperatures similar to the literature but a different method of surface treatment and activation were proposed here. Some char properties were reported and its application in dye adsorption was investigated for both adsorption kinetics and equilibrium. The three types of red dye were chosen for this study.

### 2. Research methodology

#### 2.1 Material

The material used in this study was pyrolytic char obtained from pyrolysis of waste tire rubber in a horizontal reactor at 380-420°C and under nitrogen atmosphere at 30-100 Pa (The diameter of 90% char particles was 201.84±0.88 μm). Acid Red

\*Corresponding author. Tel.: +66 2564 3001 ext.3123; fax: +66 2564 3024  
Email address: dpanu@engr.tu.ac.th  
doi: 10.14456/kkuenj.2015.34

131 ( $C_{32}H_{20}Na_2O_8S_2$ ,  $M_w=502.43$ ), Basic Red 18 ( $C_{19}H_{25}Cl_2N_5O_2$ ,  $M_w=426.34$ ) and Disperse Red 167 ( $C_{23}H_{26}ClN_5O_7$ ,  $M_w=519.93$ ) were used as model dyes. They were obtained from Hanson Chemical Co., Ltd. HCl and NaOH were supplied by Merck, Ltd., Thailand.

## 2.2 Composition analysis

The samples of as-received char were analyzed by thermogravimetric analysis (TGA) and X-ray fluorescence (XRF). In TGA analysis, a sample was placed in a platinum crucible and heated at the rate of  $10^\circ\text{C}/\text{min}$  under the ambient temperature to  $500^\circ\text{C}$  with continuous  $N_2$  flow of 50 ml/min. After that, the heating process was continued under the air atmosphere until the system reached the final temperature of  $1025^\circ\text{C}$ .

## 2.3 Morphology of char-particle surface

The sample was suspended in acetone. The colloidal system was sampled and placed on an aluminum foil before heating at  $100^\circ\text{C}$  until it was completely dried. After that, it was coated with gold before being observed with a scanning electron microscope (SEM) (Hitachi, S-3400N).

## 2.4 Adsorbent preparation

Firstly, 44 g pyrolytic tire char was soaked for 1 hr with 60%wt ethanol solution to increase its hydrophilicity by using mass ratio of char to ethanol solution of 1:5. It was then filtered, washed with distilled water and subsequently treated with 1 M HCl solution for 1 hr to remove some contaminants by using mass ratio of char to HCl solution of 1:5. The treated char was filtered and washed again with distilled water until the pH of water was constant. Then it was dried at  $100^\circ\text{C}$ . Finally, 40 gram of the obtained char was mixed with 50 ml of 60%wt ethanol solution and 40 g-NaOH dissolved in 40 ml-distilled water. After that, it was activated in a furnace at  $750^\circ\text{C}$  for 3 hrs. After activation, the char was washed with distilled water and hot water until the pH of the washing water was constant. The sample prepared through these step is called "Activated char" or "AC".

## 2.5 Pyrolytic tire char and activated char characterization

Surface area, total pore volume and pore diameter of as-received char and AC was determined by a surface area and porosity analyzer (Quantachrome, Autosorb-1). Iodine Number was carried out according to ASTM D 4607-94 (Reapproved 2011): Activated carbon, 2013, volume 15.01. The pH at the point of zero charge ( $\text{pH}_{\text{pzc}}$ ) of AC was carried out as follows: 50 ml of 0.01 M NaCl solution was placed in a closed reagent bottle. The pH was initially adjusted to a value between 2 and 12 by adding 0.1 M HCl or 0.1 M NaOH solution. Then, 0.15 gram of each sample was added and the final pH was measured after 48 hrs. The  $\text{pH}_{\text{pzc}}$  is the point that the curve of the  $\text{pH}_{\text{final}}$  vs.  $\text{pH}_{\text{initial}}$  intersects with the curve of  $\text{pH}_{\text{initial}} = \text{pH}_{\text{final}}$ .

## 2.6 Adsorption experiment

Three types of dye, Acid Red 131, Basic Red 18 and Disperse Red 167, were used to evaluate the adsorption

capacity. First, dye solutions with the concentration between 10-50 ppm were prepared for adsorption kinetics and equilibrium studies. 0.029 g AC was added into 30 ml dye solution and the mixture was shaken in a shaker at 75 rpm and at  $26^\circ\text{C}$ . After that AC was removed from the remaining dye solution by centrifugation at 5000 rpm for 2 min. The dye concentrations at many time intervals were measured using a spectrophotometer (UNICO, UV-1200) to obtain the kinetic data. The absorbance was read at the wavelength of 560, 490 and 465 nm for Acid Red 131, Basic Red 18 and Disperse Red 167, respectively. Equilibrium adsorption was achieved by leaving the solution shaken up to 50 hrs, 54 hrs and 1 hr for Acid Red 131, Basic Red 18 and Disperse Red 167, respectively and then the final concentrations of the solutions were measured. Adsorption capacity is defined as

$$q_t = \frac{(C_0 - C_t) \times V}{w} \quad (1)$$

$$q_e = \frac{(C_0 - C_e) \times V}{w} \quad (2)$$

Where  $q_t$  and  $q_e$  are the adsorption capacity (mg/g) at any time and at equilibrium, respectively,  $C_0$  is the initial dye concentration (mg/l),  $C_t$  and  $C_e$  are dye concentrations at any time and at equilibrium (mg/l),  $V$  is the volume of solution (ml) and  $w$  is the mass of activated char (g).

## 3. Results and discussion

### 3.1 Composition analysis

The composition of as-received char obtained from TGA and XRF is shown in Table 1. The results showed that the char contained mostly carbon as high as 81.81% since rubber molecule is hydrocarbon and the rubber composite is filled with carbon black. Sulfur was found to be 2.3% in the char since it is used to vulcanize the rubber composite. Total ash contributes 13.62% of the char including 1.17% silica which is used as filler and 3.11% zinc which is from the activator for vulcanization.

### 3.2 Morphology and functional groups

SEM micrograph of as-received char was shown in Figure 1. It was observed that pyrolytic tire char particles are fine and spherical. The particle size from an image analyzer program expressed that the diameter of pyrolytic tire char was  $96 \pm 26$  nm. FTIR spectra of char and AC were shown in Figure 2. The peaks at  $3455.81$  and  $1631.48 \text{ cm}^{-1}$  of the char were observed corresponding to  $-\text{OH}$  (hydroxyl) and  $\text{COO}^-$  (carboxylates), respectively. After activation, the peaks of AC were slightly shifted to  $3443.59$  and  $1632.00 \text{ cm}^{-1}$ , respectively.

### 3.3 Pyrolytic tire char and activated char characterization

Surface area, total pore volume and pore diameter of as-received char and AC obtained from a surface area and porosity analyzer, iodine number and  $\text{pH}_{\text{pzc}}$  are shown in Table 2.

**Table 1** The composition of as-received char

Composition from TGA	Element from XRF	%
Volatile matter		4.57
Carbon		81.81
Ash	O	6.01
	Zn	3.11
	S	2.3
	Si	1.17
	Ca	0.48
	Fe	0.13
	K	0.11
	Al	0.1
	Br	0.05
	Mg	0.04
	P	0.04
	Cl	0.03
	Ti	0.02
	Co	0.01
Cu	0.01	
Pb	0.01	

13.62

**Table 2** Surface area, total pore volume and pore diameter of Char and AC

Sample	Surface Area (m <sup>2</sup> /g)	Total Pore Volume (ml/g)	Pore Diameter (°A)	Iodine number (mg/g)	pH <sub>pzc</sub>
Char	154.7	1.251	323.4	95	n/a
Ac	228.9	1.999	349.3	137	7.4

n/a = not available

The results expressed that the specific surface area (SSA) and total pore volume of activated char (AC) increased from 154.7 to 228.9 m<sup>2</sup>/g and from 1.251 to 1.999 ml/g, respectively, whereas the pore size increased slightly from 323.4 to 349.3 °A after activation. According to Mui et al. [6, 11], as-received pyrolytic tire char had SSA of 122 m<sup>2</sup>/g which was increased to 168 m<sup>2</sup>/g after CO<sub>2</sub> activation at 923°C higher than temperature applied in this work. Besides, total pore volume of their activated char was 0.123 ml/g which was lower than ours. Therefore, it seems that even at a higher temperature, physical activation by CO<sub>2</sub> could increase SSA by 37% while chemical activation by NaOH solution in our case could increase SSA by 48%.

In addition, it was observed that iodine number of char activated with NaOH in a furnace at 750°C was increased from 95 to 137 mg/g due to an increase of its surface area. However, both SSA and iodine number were still lower than the standard of activated carbon (1000 m<sup>2</sup>/g) probably attributable to highly hydrophobic surfaces of very fine char powder (as small as 100 nm). For the determination of pH<sub>pzc</sub>, it was found that pH<sub>pzc</sub> of AC was about 7.4 while pH<sub>pzc</sub> of as-received char could not be determined due to its inability to be well mixed with water.

**3.4 Adsorption kinetics**

Adsorption capacities at many intervals of acid dye (AR131), basic dye (BR18), disperse dye (DR167) with average initial pH of dye solution of 5.85, 6.74 and 6.87, respectively were shown in Figure 3. When the initial concentration was lower, *q<sub>t</sub>* of acid dye (AR131) and basic dye (BR18) can reach their equilibrium faster. In addition, *q<sub>e</sub>* of all dyes were increased with increasing initial dye concentration as can be seen in Table 3.

The pseudo-first-order Lagergren model and the pseudo-second-order model are expressed as Eq. (3) and (4), respectively. The former implies that kinetics is governed by the available adsorption sites while the latter depends both on the amount of adsorbates and the availability of adsorption sites on the adsorbents.

$$\ln(q_e - q_t) = \ln(q_e) - k_1 t \tag{3}$$

$$\frac{t}{q_t} = \frac{1}{k_2 q_e^2} + \frac{1}{q_e} t \tag{4}$$

Where *q<sub>t</sub>* and *q<sub>e</sub>* were already defined. *k<sub>1</sub>* and *k<sub>2</sub>* are the rate constants of the pseudo-first-order adsorption (min<sup>-1</sup>) and the pseudo-second-order adsorption (gm<sup>-1</sup>min<sup>-1</sup>), respectively.

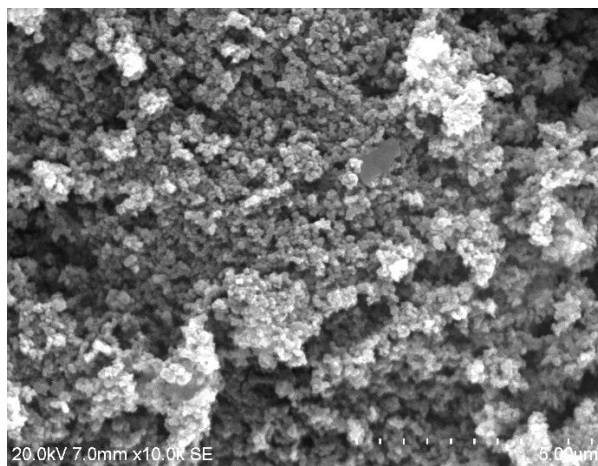


**Figure 1** SEM micrograph of as-received char

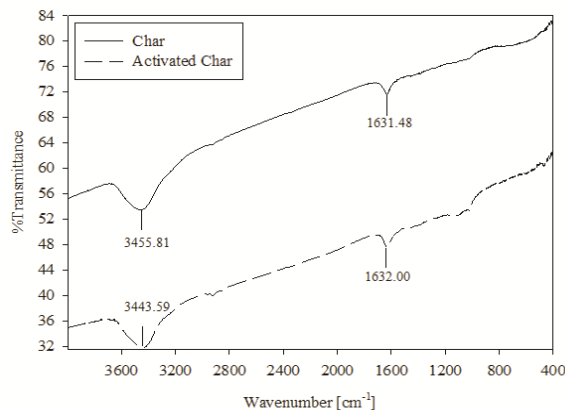


**Figure 2** FT-IR spectra of char and AC

The values of  $k_1$ ,  $k_2$  and  $R^2$  of both models for acid dye (AR131), basic dye (BR18) and disperse dye (DR167) are presented in Table 4. As can be seen, considering higher value of  $R^2$ , adsorption of all dyes by using the activated char could be better explained by the pseudo-second-order model. Similar findings were reported before for the adsorption of methylene blue on activated carbons [12]. The results revealed that  $q_e$  obtained from pseudo-second-order of all three dyes was increased with increasing the initial concentration of dyes, implying the availability of adsorptive sites.

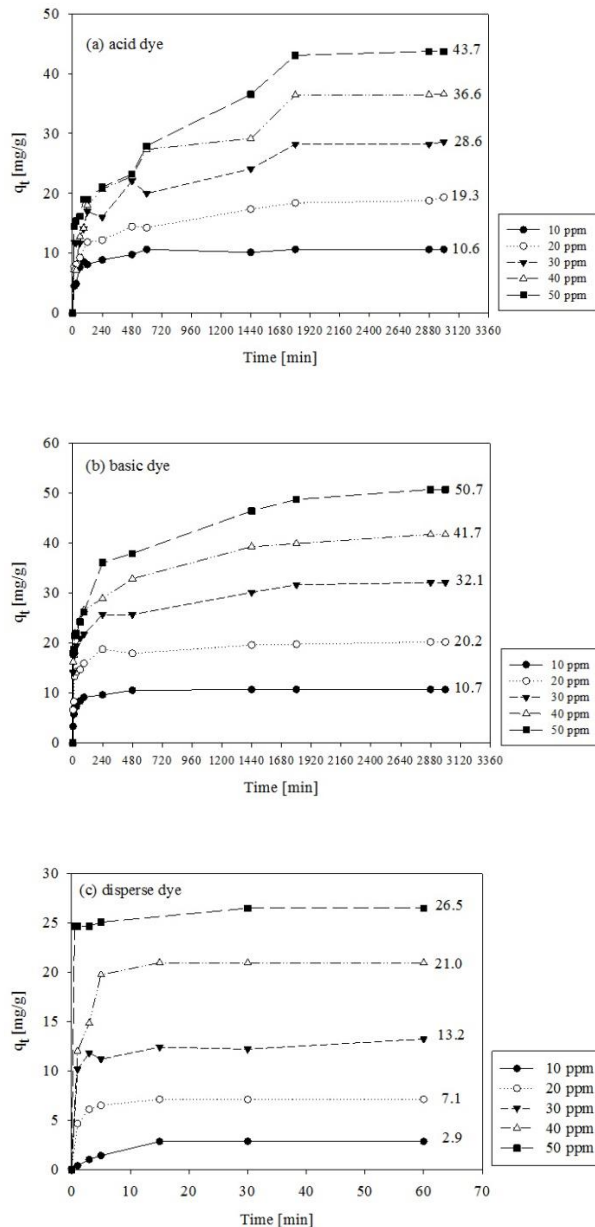


**Figure 3** Adsorption kinetics for (a) acid dye (AR131), (b) basic dye (BR18) and (c) disperse dye (DR167)

In addition, when the initial concentration of dye increased from 10 to 50 ppm, the rate constants,  $k_2$ , decreased from 0.0028 to 0.0001  $\text{g mg}^{-1}\text{min}^{-1}$  and 0.0073 to 0.0003  $\text{g mg}^{-1}\text{min}^{-1}$  for adsorption of acid dye and basic dye, respectively implying that adsorption rates of basic dye was faster than those of acid dye. Regarding adsorption for disperse dye,  $k_2$  did not show definite trend because disperse dye (DR167) cannot be dispersed well in water without any dispersing agent.

### 3.5 Adsorption equilibrium

Adsorption percentage at equilibrium of acid dye (AR131), basic dye (BR18) and disperse dye (DR167) can be calculated according Eq. (5)

$$\% \text{adsorption} = \frac{(C_0 - C_e)}{C_0} \times 100 \quad (5)$$

In Figure 4, at the initial dye concentrations of 10, 20, 30, 40 and 50 ppm, It was found that basic dye (BR18) can be totally adsorbed by AC, acid dye (AR131) was highly adsorbed with percentage of 88.2 – 100, and disperse dye (DR167) was adsorbed with percentage of 26.9 – 50.7. When the initial concentration of dye was increased, the adsorption percentage of acid dye decreased due to the limited number of adsorbent pores. On the other hand, when the initial concentration of disperse dye (DR167) was increased, the adsorption percentage increased. Probably, at a low initial concentration, dye molecules could not be totally dispersed and they formed aggregates so they cannot be well adsorbed in adsorbent pores. Whereas, a higher initial concentration could promote the probability of dye molecules to be in contact with adsorbent pores so the adsorption percentage could be increased.

Since the adsorption percentage of basic dye (BR18) was 100% when the initial dye concentration was 10 – 50 ppm, its isotherm could not be obtained. Therefore, another experiment was performed at higher concentrations which were 86, 108, 137, 156, 168 and 213 ppm. The remaining concentration was measured with spectrophotometer after shaking at a speed of 75 rpm at 26°C for 54 hrs.

In order to study equilibrium adsorption, Freundlich isotherm and Langmuir isotherm were applied to the results. Normally, the empirical Freundlich isotherm is applied for the results that have not reached the saturation so it shows a still increasing trend of the isotherm. Whereas, Langmuir implies a monolayer adsorption with limited localized adsorption sites so finally the adsorption will reach a saturation point.

**Table 3** Adsorption capacities at equilibrium of acid dye (AR131), basic dye (BR18) and disperse dye (DR167)

Dye	$q_e$ mg/g				
	10 (ppm)	20 (ppm)	30 (ppm)	40 (ppm)	50 (ppm)
Acid	10.6	19.3	28.6	36.6	43.7
Basic	10.7	20.2	32.1	41.7	50.7
Disperse	2.9	7.1	13.2	21.0	26.5

**Table 4** Parameters obtained from pseudo-first-order and pseudo-second-order kinetic models

Dye	Initial concentration (ppm)	Pseudo-first-order			Pseudo-second-order		
		$q_e$ (mg/g)	$k_1$ ( $\text{min}^{-1}$ )	$R^2$	$q_e$ (mg/g)	$k_2$ ( $\text{g mg}^{-1} \text{min}^{-1}$ )	$R^2$
Acid dye	10	4.07	0.0017	0.6729	10.7	0.0028	0.9997
	20	10.77	0.0011	0.9387	19.4	0.0006	0.9961
	30	17.72	0.0015	0.8873	28.5	0.0003	0.9901
	40	30.38	0.0021	0.8818	37.7	0.0002	0.9894
	50	35.07	0.0017	0.8604	45.5	0.0001	0.9831
Basic dye	10	5.33	0.0080	0.7026	10.7	0.0073	0.9999
	20	7.41	0.0017	0.7700	20.2	0.0021	0.9997
	30	15.37	0.0018	0.9073	32.36	0.0007	0.9989
	40	22.32	0.0015	0.9301	42.02	0.0004	0.9985
	50	24.39	0.0044	0.8772	51.28	0.0003	0.9979
Disperse dye	10	2.46	0.0657	0.9983	3.19	0.0602	0.9925
	20	5.18	0.4663	0.9217	7.19	0.3252	0.9999
	30	3.56	0.0564	0.4202	13.33	0.0792	0.9994
	40	5.20	0.0377	0.4169	21.28	0.0706	0.9997
	50	5.65	0.3411	0.3304	26.53	0.2538	1.0000

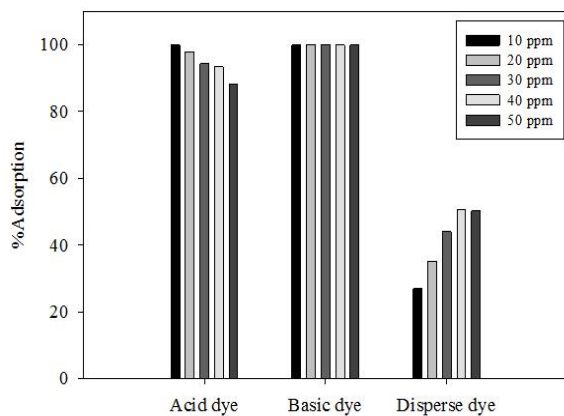


**Figure 4** Adsorption percentage at equilibrium of acid dye (AR131), basic dye (BR18) and disperse dye (DR167)

Freundlich isotherm is expressed as Eq (6)

$$q_e = K_F C_e^{1/n} \tag{6}$$

or in the linear form as

$$\ln q_e = \ln K_F + \frac{1}{n} \ln C_e \tag{7}$$

Here,  $K_F((\text{mg/g}_{AC})(\text{l/mg})^{1/n})$  and  $n$  are Freundlich parameters. Higher value of  $K_F$  implies higher adsorption capacity. Langmuir isotherm is written as

$$\frac{C_e}{q_e} = \frac{1}{q_m} C_e + \frac{1}{K_L q_m} \tag{8}$$

Here,  $q_m$  and  $K_L$  are a maximum monolayer adsorption capacity (mg/g) and Langmuir constant (l/mg).

The parameters obtained from Freundlich isotherm and Langmuir isotherm are collected in Table 5. It can be seen that adsorption of acid dye (AR131) and basic dye (BR18) using AC was consistent with Langmuir equation. The results of acid dye (Eriony Navy R) and basic dye (Astrazon Brilliant Red 4G) adsorption by using commercial activated carbon (Norit GAC 1240 PLUS) without any treatment at initial concentration between 50-1000 ppm was also reported to follow Langmuir isotherm [13].

In general, adsorption of molecules or ions on the adsorbent surfaces is governed by the attractive forces among them, which could be dispersive forces or Van der Waals forces and electrostatic interaction. If the electrostatic interactions were the main adsorption mechanism, the adsorption ability depends on relative values of  $\text{pH}_{\text{pzc}}$  and  $\text{pH}$  of the solution. At  $\text{pH} > \text{pH}_{\text{pzc}}$ , the carbon surface becomes negatively charged so it prefers to adsorb cationic species. In contrast, at  $\text{pH} < \text{pH}_{\text{pzc}}$ , the carbon surface becomes positively charged so it prefers to adsorb anionic species [14]. One of the examples is the work of Jindarom *et al.* [15]. They reported that char obtained from pyrolysis of sewage sludge at 350-750°C with  $\text{pH}_{\text{pzc}}$  9.31-9.74

**Table 5** Freundlich and Langmuir parameters for adsorption

Isotherm	Parameters	Dye		
		Acid	Basic	Disperse
Langmuir	$n$	3.3	6.0	0.1
	$K_F ((\text{mg/g}_{AC})(\text{l/mg})^{1/n})$	25.94	68.09	0.53
	$R^2$	0.9796	0.8816	0.9845
	$q_m (\text{mg/g}_{AC})$	49.8	138.9	-10.6
	$K_L (\text{l/mg})$	1.14	0.28	0-0.03
	$R^2$	0.9854	0.9948	0.8387



could adsorb basic dye (Astrazon blue FGGL), which is a cation, and acid dye (Telon light yellow), which is an anion, with  $q_m$  of 212.77-416.67 and 12.71-71.43 mg/g, respectively [15].

In our work, the activated char had  $pH_{pzc}$  of 7.4 which was higher than  $pH$  of dye solutions so its surface should be positively charged and it should prefer the adsorption of acid dye which is an anion to the adsorption of basic dye which is a cation. The opposite was observed since for basic dye was greater. The mechanism of adsorption should then be from dispersive forces or Van der Waals forces between dye molecules and char surfaces [16]. Considering molecular weight of the dyes, Basic Red molecules are smaller which may be accommodated in the pore of AC more easily. The negligible effect of electrostatic forces was also seen from the work of Faria *et al.* [15]. When the initial  $pH$  of dye solution was 6-7, a commercial activated carbon with  $pH_{pzc}$  of 9.7 could adsorb basic dye (Astrazon Brilliant Red 4G) with  $q_m$  higher than acid dye (Eriony Navy R).

For disperse dye (DR167), it was found that  $R^2$  of fitting with Freundlich equation was higher than Langmuir equation. Some Langmuir parameters were found negative which was not possible implying that Freundlich isotherm is more suitable to describe this system. Our results did not follow Langmuir equation may be because disperse dye (DR167) cannot be dispersed well in water without any dispersing agent as discussed before and so the adsorptive sites were not almost used up so the behavior of monolayer adsorption was not observed. Therefore, it can be concluded that for disperse dye, the data were better fit with Freundlich equation.

#### 4. Conclusion

In this research, pyrolytic tire char was treated with ethanol to increase its hydrophilicity, treated with HCl solution to remove some contaminants, and then activated with NaOH in a furnace at 750°C to increase its specific surface area (SSA). After treatment, SSA and iodine number were increased while the pore size slightly increased. It seems that surface hydrophobicity of the fine pyrolytic char particles is a major obstacle to an increase in SSA.

For adsorption kinetics, when the solution concentration was varied to be 10 – 50 mg/L, the results were more consistent with the pseudo-second-order model than pseudo-first-order model. The adsorption rate constant,  $k_2$ , showed that kinetics for acid dye (AR131) was slower than basic dye (BR18) whereas kinetics for disperse dye (DR167) was much slower and did not show a definite trend. For adsorption equilibrium, the adsorption isotherms for acid dye (AR131) and basic dye (BR18) followed Langmuir equation but that for disperse dye (DR167) was better fit with Freundlich equation. The activated char could remove basic dye with higher efficiency than acid dye.

#### 5. Acknowledgments

The financial support from Thammasat University together with National Research Council of Thailand for the fiscal year 2014 is highly acknowledged.

#### 6. References

- [1] Vakili M, Rafatullah M, Salamatinia B, Abdullah AZ, Ibrahim MH, Tan KB, Gholami Z, Amouzgar P. Application of chitosan and its derivatives as adsorbents for dye removal from water and wastewater: A review. *Carbohydr. Polym* 2014;113:115-130.
- [2] Zhou K, Zhang Q, Wang B, Liu J, Wen P, Gui Z, Hu Y. The integrated utilization of typical clays in removal of organic dyes and polymer nanocomposites. *J Clean Prod* 2014;81:281-289.
- [3] Noorimotlagh Z, Soltani RDC, Khataee AR, Shahriyar S, Nourmoradi H. Adsorption of a textile dye in aqueous phase using mesoporous activated carbon prepared from Iranian milk vetch. *J Taiwan Inst Chem.Eng* 2014;45:1783-1791.
- [4] Gupta VK, Nayak A, Agarwal S, Tyagi I. Potential of activated carbon from waste rubber tire for the adsorption of phenolics: Effect of pre-treatment conditions. *J Colloid Interf Sci* 2014;417:420-430.
- [5] Danwanichakul P, Danwanichakul D. Mass transfer analysis of Mercury(II) removal from contaminated water by non-porous waste tire granules. *Eur J Sci Res* 2009;36:363-375.
- [6] Mui ELK, Cheung WH, Valix M, McKay G. Mesoporous activated carbon from waste tyre rubber for dye removal from effluents. *Micropor Mesopor Mat* 2010;130:287-294.
- [7] Wang L. Application of activated carbon derived from 'waste' bamboo culms for the adsorption of azo disperse dye: Kinetic, equilibrium and thermodynamic studies. *J Environ Manage* 2012;102:79-87.
- [8] Yamkaya P, Danwanichakul D, Danwanichakul P. Effect of filling surface-treated pyrolytic char on resistivity of rubber films. *KKU Engineering Journal* 2015;42(1):91-99. (In Thai).
- [9] Quek A, Balasubramanian R. Removal of copper by oxygenated pyrolytic tire char: Kinetics and mechanistic insights. *J Colloid Interf Sci* 2011;356:203-210.
- [10] Quek A, Vijayaraghavan K, Balasubramanian R. Methylene Blue Sorption onto Oxygenated Pyrolytic Tire Char: Equilibrium and Kinetic Studies. *J Environ Eng* 2011;137:833-841.
- [11] Mui ELK, Cheung WH, McKay G. Tyre char preparation from waste tyre rubber for dye removal from effluents. *J Hazard Mater* 2010;175:151-158.
- [12] Wang S, Zhu Z.H. Effects of acidic treatment of activated carbons on dye adsorption. *Dyes Pigments* 2007;75:306-314.
- [13] Faria PCC, Órfão JJM, Pereira MFR. Adsorption of anionic and cationic dyes on activated carbons with different surface chemistries. *Water Res* 2004;38:2043-2052.
- [14] Rodríguez-reinoso F. The role of carbon materials in heterogeneous catalysis. *Carbon* 1998;36:159-175.
- [15] Jindarom C, Meeyoo V, Kitiyanan B, Rirksoomboon T, Rangsunvigit P. Surface characterization and dye adsorptive capacities of char obtained from pyrolysis/gasification of sewage sludge. *Chem Eng J* 2007;133:239-246.
- [16] Radovic LR, Silva IF, Ume JI, Menéndez JA, Leon CA, Scaroni AW. An experimental and theoretical study of the adsorption of aromatics possessing electron-withdrawing and electron-donating functional groups by chemically modified activated carbons. *Carbon* 1997;35:1339-1348.